1. Joanna MICHAŁOWSKA[1], 2. Paweł TOMIŁO[2]

Lublin University of Technology, Faculty of Electrical Engineering and Computer Science (1)
Lublin University of Technology, Faculty of Management (2)
ORCID: 1. 0000-0002-2353-6305; 2. 0000-0003-4461-3194

doi:10.15199/48.2025.01.56

Determination of the typical course values of aircraft parameters for the new measurement system in the case of aircraft take-off and landing

Abstract. *The measurements were carried out in a PZL 110 Koliber 150 aircraft using two specially developed measurement systems.The first system uses an Inertial Measurement Unit with 9 degrees of freedom (accelerometer, magnetometer, gyroscope). The second measurement system is based on the use of a logarithmic power detector together with an antenna and microcontroller board. An algorithm was developed that uses an artificial neural network with a variational autoencoder architecture with LSTM layers. Empirical relationships describing the acceleration in three axes, the Euler angle, and the electric scale of the electromagnetic field were observed. It has been demonstrated on the basis of the conducted research that the use of the developed artificial neural network model will be used to generate generalized time courses of the analyzed flight parameters. This type of tool has potential use in pilot training, due to critical factors occurring during the takeoff and landing phases.*

Streszczenie *Pomiary przeprowadzono w samolocie PZL 110 Koliber z wykorzystaniem opracowanych specjalistycznych dwóch systemów pomiarowych. Pierwszy system wykorzystuje jednostkę pomiaru bezwładnościowego z 9 stopniami swobody (akcelerometr, magnetometr, żyroskop). Drugi system pomiarowy opiera się na wykorzystaniu logarytmicznego detektora mocy wraz z anteną i płytką mikrokontrolera. Opracowano algorytm, który wykorzystując sztuczną sieć neuronową o architekturze wariacyjnego autoenkondera z warstwami LSTM. Zaobserwowano zależności emiryczne opisujace akceleracje w trzech osiach, kąt Eulera oraz składaową elektryczną pola elektromagnetycznego. Wykazano na przykładzie przeprowadzonych badań, ze wykorzystanie opracowanego modelu sztucznej sieci neuronowej posłuży do wygenerowania uogólnionych przebiegów czasowych analizowanych parametry lotu. Tego typu narzędzie ma potencjalne zastosowanie w szkoleniu pilotów, ze względu na czynniki krytyczne występujące podczas faz startu i lądowania (**Określenie typowych wartości parametrów kursu samolotu dla nowego układu pomiarowego w przypadku startu i lądowania samolotu**).*

Słowa kluczowe: Sztuczna sieć neuronowa, Wariacyjny AutoEnkoder, Statek powietrzny, Inercyjna jednostka pomiarowa, Pole Elektromagnetyczne
Keywords: Artificial Neural Network, Variational AutoEncoder, Aircraft, Inertial Measurement Unit, Electromagnetic Field

Introduction

Monitoring flight parameters is a very important research aspect, especially during training flights. Current pilot training standards lead to a continuous effort to improve the level of safety. For many years, various types of recording devices have been installed in aircraft to analyse aviation incidents. The European Aviation Safety Agency (EASA) recommends the need to conduct research into monitoring flight parameters.

Such actions lead to improved safety as well as increased quality of training. In addition, there are also reports that the influence of high-frequency sounds may impair cognitive abilities. Large-scale electronic avionics systems are considered to be the source of rapidly changing fields. These fields are also propagated from external sources. Putting low-cost prototype measurement systems on aircraft allows for data monitoring as a common way to improve safety [1-3]. Artificial intelligence and neural networks have great potential to perform detailed analyses concerning the recognition of aspects of flight parameters, such as: acceleration [4,5], Euler angles and the electric component of the electromagnetic field (E_{RMS}).

Materials and methods

For Two sensor measurement systems were placed in the PZL 110 Koliber 150 aircraft - an inertial measurement system with 9 degrees of freedom and an electromagnetic field. Indications from both systems were collected for the moment the aircraft took off and landed. Measurements were made under varying weather conditions with temperatures ranging from 18 to 24 °C and wind velocities ranging from 5 to 29 Knots. The first developed authors system uses an Inertial Measurement Unit with 9 degrees of freedom (accelerometer, magnetometer, gyroscope). The indications are converted to linear acceleration with respect to the coordinate system and to Euler angles. The processed data are stored in the Data Processing Unit. A new form of the second measurement system was proposed is based on the use of a logarithmic power detector together with an antenna and microcontroller board. Data from the system is stored on a smartphone device. This study is a continuation of the research described in references [6,7]. The principle of the system using IMU is shown in Figure 1 and the system measuring E_{RMS} is shown in Figure 2.

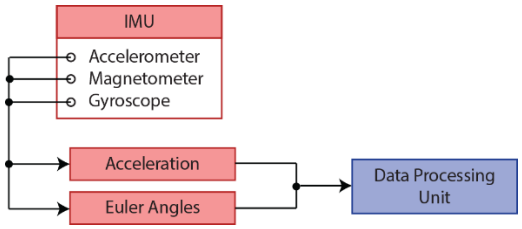

Fig. 1. Principle of the measurement system using IMU

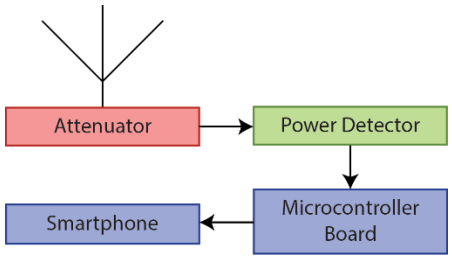

Fig. 2. Principle of the measurement system E_{RMS}

A photo of the device used to measure acceleration and Euler angles is shown in Figure 3a, while Figure 3b shows the device used to measure E_{RMS}.

The data were used to train the developed a generated artificial neural network model, on the basis of the results of

which typical time courses of acceleration values, Euler angles and electromagnetic field values were indicated for time series covering the moment of aircraft takeoff and landing. Developed algorithm can serve as a system for detecting irregularities in timeseries of 3-axis acceleration and Euler Angles and occurrences of electromagnetic field outliers in the takeoff and landing procedure.

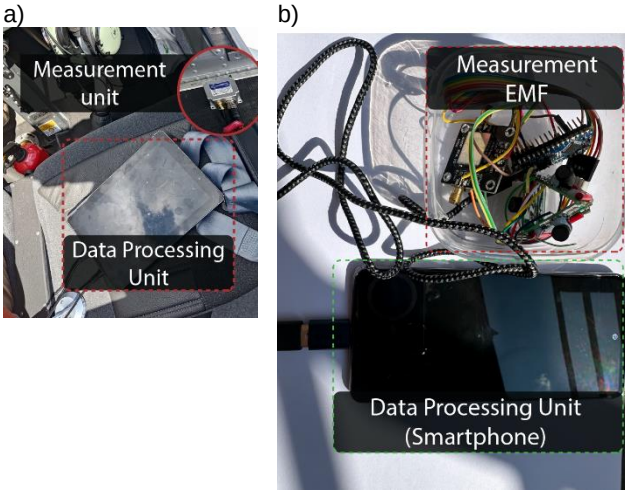

Fig. 3. a) Acceleration and Euler angles measurement device, b) E_{RMS} measurement device

First, in order to create a larger dataset that will allow the generalized signal characteristics to be determined later in the analysis, a generative artificial neural network model based on the variational autoencoder (VAE) architecture was developed.

To analyze the occurrence of outliers from the generalized time-series for a given value, a method similar to Piecewise Aggregate Approximation (PPA) was used [8-10]. Similar to the PPA method, dimensionality reduction was applied by using divide the original time-series $X = (x_1, \dots, x_M)$ into equally sized frames $X' = (x'_1, \dots, x'_2)$.. The dimension is reduced from n to M by using equation (1).

$$\bar{X}_i = \frac{M}{n} \sum_{j=\frac{n}{N}(i-1)+1}^{\left(\frac{n}{M}\right)\cdot i} x_j \tag{1}$$

For each frame created, the median was determined, as well as two intervals from the first quartile (Q1) to the third quartile (Q3) and from the same interval will increase by 1.5 the inter-quartile range (IQR). The second interval is assumed to be the interval of acceptable values, which means that values outside this interval are counted as outliers. Figure 1 shows an example of determining the occurrence of outliers for an E_{RMS} time series.

Data generation with LSTM VAE with positional encoding

Due to the number of samples in the data set, as well as the possible presence of noise, it was decided to use a Variational AutoEncoder (VAE) architecture. This type of artificial neural network model allows both the generation of new data based on learned features and allows the removal of anomalies present in the data. VAE is a type of generative machine learning model that combines ideas from probability theory and deep learning. This model uses two main elements in its architecture are: Encoder and Decoder. The Encoder is responsible for mapping the input data into a latent space. The Encoder generates the parameters of the normal distribution μ - the mean and σ - the standard deviation [2]. The developed model architecture uses Logn-Short Term Memory (LSTM) layers. The LSTM is based on a gate mechanism that consists of the following elements [11-12]:

- g_c - input node;
- i_t – input gate;
- f_t – forget gate;
- o_t –output gate;
- s_t – internal state.

The information processing process using the LSTM layer was described by equations (2-7):

$$g_t = \phi(W^{g_x} x_t + W^{g_h} h_{t-1} + b_g) \tag{2}$$
$$i_t = \sigma(W^{i_x} x_t + W^{i_h} h_{t-1\_} b_1) \tag{3}$$
$$f_t = \sigma(W^{f_x} x_t + W^{f_h} h_{t-1\_} b_f) \tag{4}$$
$$o_t = \sigma(W^{o_x} x_t + W^{o_h} h_{t-1} + b_o) \tag{5}$$
$$s_t = g_t \odot i_t + s_{t-1} \odot f_t \tag{6}$$
$$h_t = \phi(s_t) \odot o_t \tag{7}$$

where:

t – given time
x – input data;
W – weights created in the training process;
b – bias created in the training process;
$\odot$ - pointwise multiplication.

According to [13,14], a positional encoding operation was applied to data input to the LSTM layer to improve the model's ability to reproduce data.

The developed model architecture in the encoder architecture first uses linear projection to increase the dimensionality of the data and give it positional encoding. In the next step, the data passes through the LSTM layer, from which σ and μ parameters are obtained as a result of 2 different linear projection. Based on these parameters, the input values z for the decoder are sampled (Gaussian Distribution). In the decoder, linear projection was used in the first layer, followed by an LSTM layer with positional encoding. The tensor returned from this layer using linear projection is processed into a vector that is the reconstructed input data. The architecture in question is shown in Figure 4.

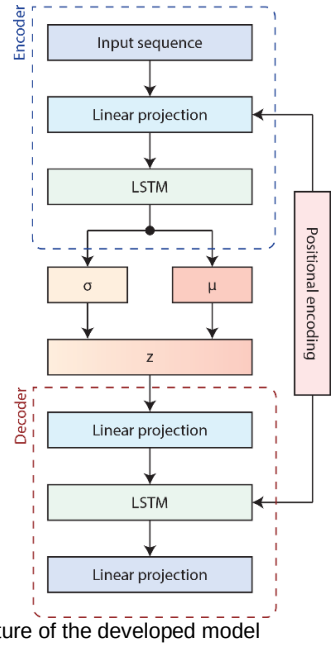

Fig. 4. Architecture of the developed model

The sum of the Kullback-Leibler divergence ($\mathcal{L}_{KLD}$) and Mean Square Error ($\mathcal{L}_{MSE}$) functions for the reconstructed data was used as the model's loss function. The functions were sequentially represented by equation (8) and (9).

$$\mathcal{L}_{KLD} = -0.5 \cdot \sum 1 + \log(\sigma) - \mu^2 - e^{\log(\sigma)} \tag{8}$$

$$\mathcal{L}_{MSE} = \frac{1}{n}\sum l_n, \qquad l_n = (x_n - y_n)^2 \tag{9}$$

where:

n – number of samples;

x_n – input data at position n;

y_n – output data (reconstructed x_n) at position n.

The use of a metric in the form of $\mathcal{L}_{KLD}$ is a form of regularization that forces the latent space to adopt a standardized shape. This prevents the occurrence of a degenerate distribution in the latent space. The $\mathcal{L}_{MSE}$ function is responsible for comparing the reconstructed values with the input values.

A separate model was created for each time series. For signals in the form of acceleration and Euler angles, time series were used:

- For landing: 3000 samples until the aircraft stops
- In the case of takeoff: 3000 samples after the aircraft takes off.

For indications from the electromagnetic field sensor, 60 samples were used due to the different sampling frequency of the two systems. The indications of both systems correspond to a time of 1 minute. In each case, the number of iterations of training the model was 800. For the model that reconstructs the E_{RMS}, a lower number of model hyperparameters was used due to the smaller number of samples falling within the 1-minute time frame. The course of the loss function values for each of the developed models is shown in Figure 5.

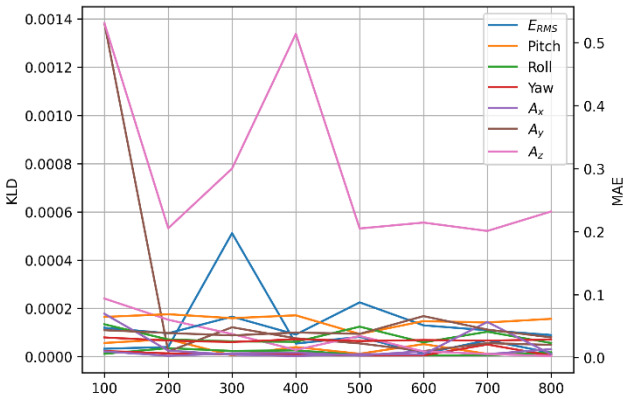

Fig. 5. The course of the loss function values for each of the developed models

Each model was selected the iteration for which the model obtained the smallest value of the loss function. It can be seen from the above graph that the model did the worst in generalizing the values from the acceleration time courses on the z-axis - A_z.

Results

Based on the generated time courses and the actual time courses, "frames" were created, in which the previously presented values from the modified PPA method were determined. A single frame consists of 100 samples.In the case of the landing phase for the time course of the pitch angle values, initial larger fluctuations in the values are noticeable until they stabilize. For the Roll angle, the median values take on an uneven distribution, which is close to 0 in the last frame.For the Yaw angle, standardization using z-score was applied, due to the fact that this value is dependent on magnetic north. The course of this value is also initially characterized by larger fluctuations, which cease. For the acceleration value, there is a noticeable increase in deviations around frame 19, where, on average, the moment of touchdown occurred, followed by the movement of the aircraft along a runway with a ground surface. The time courses with superimposed frames and box plots are shown in Figure 6.

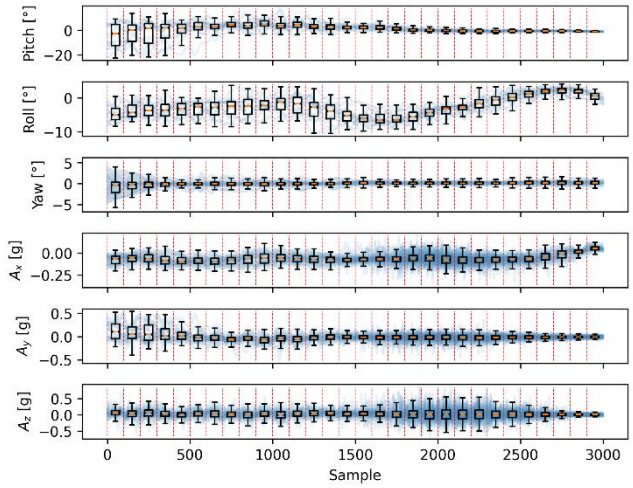

Fig. 6. The time courses with superimposed frames and box plots

For E_{RMS} values, a single frame consists of 10 samples. This is due to the sampling frequency of the device. Due to the small number of frames, the data for each frame is shown in Table 1, while the Time Course with superimposed frames and box plots are shown in Figure 7.

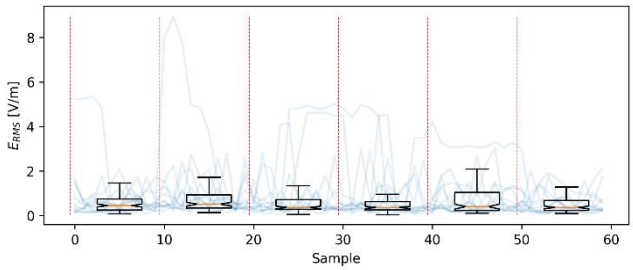

Fig. 7. The time courses with superimposed frames and box plots for E_{RMS}

Table 1. Summary of values obtained for the E_{RMS} time series

Frame	Q1-1.5IQR	Q1	Q3	Q3+1.5IQR
1	0.081	0.24850	0.381546	1.466
2	0.135	0.33850	0.432120	1.723
3	0.044	0.27775	0.302223	1.341
4	0.039	0.25525	0.312880	0.960
5	0.100	0.22925	0.290102	2.093
6	0.084	0.23100	0.303155	1.283

Exactly the same procedure was carried out for the takeoff phase. For the pitch angle, the opposite characteristic to the landing is noticeable. The values initially maintain a small variation, but in the final phase there is a larger deviation. In the case of the Roll angle, there is a kind of periodicity for the deviations, but this may be related to the influence of the wind. The Yaw angle again shows the opposite characteristics relative to the landing, initially the values are stable, and in the final phase there is a large variation. Acceleration on the x and y axes also shows an

inverse behavior relative to landing. In contrast, acceleration on the z-axis is characterized by a fairly high stability relative to the other time courses. The time courses with superimposed frames and box plots are shown in Figure 8.

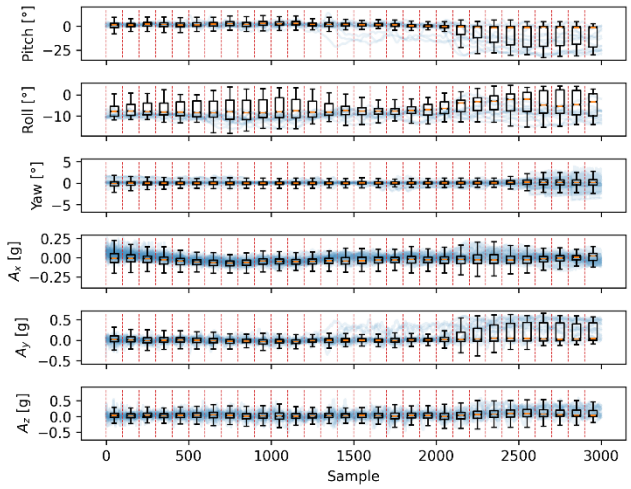

Fig. 8. The time courses with superimposed frames and box plots

In the case of E_{RMS}, there are much larger median values as well as deviations during landing. The data for each frame is shown in Table 2, while the Time Course with superimposed frames and box plots are shown in Figure 9.

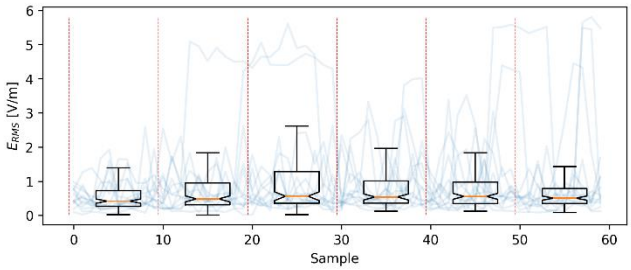

Fig. 9. The time courses with superimposed frames and box plots for E_{RMS}

Table 2. Summary of values obtained for the E_{RMS} time series

Frame	Q1-1.5IQR	Q1	Q3	Q3+1.5IQR
1	0.021	0.268	0.354469	1.391
2	0.015	0.311	0.395217	1.835
3	0.018	0.355	0.433751	2.613
4	0.121	0.358	0.450375	1.965
5	0.122	0.345	0.470388	1.834
6	0.087	0.346	0.444413	1.431

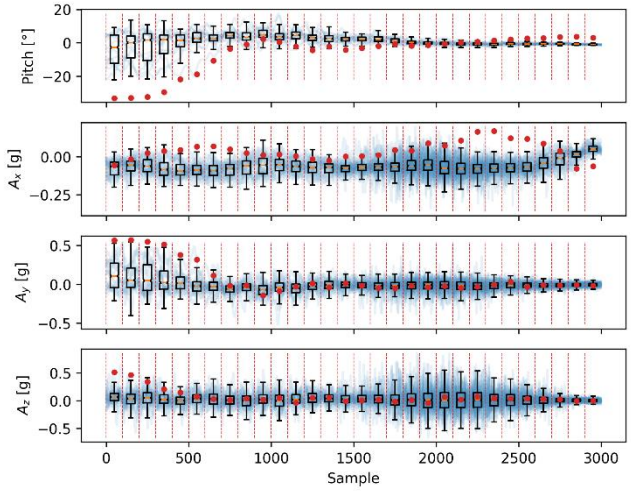

Fig. 10. Example of the landing technique value course

Tests were performed to demonstrate the correctness of the selected model. A pilot with less experience sat behind the aircraft's controls, which made it possible to compare the results obtained from the models in order to check the elements requiring improvement in takeoff and landing techniques. An example of the landing technique value course is shown in Figure 10 (only values that fall outside the range are included).

Based on the example, it can be concluded that the pilot lowered the flight too quickly, with too small an angle of Pitch. At the same time, the acceleration in the y-axis was too high, and also the course of acceleration values on the x-axis is out of generalized values in places. There were also anomalies in the E_{EMF} values. The first occurred near the execution of the flare maneuver, while the next two occurred moments before the aircraft's touchdown. The course of the values in question is shown in Figure 11.

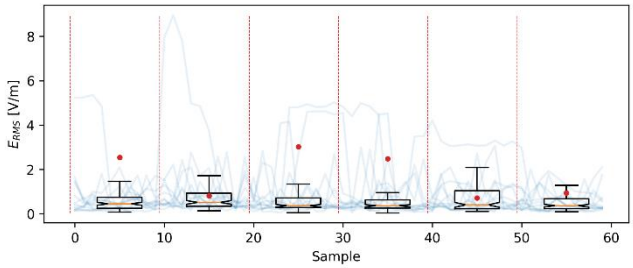

Fig. 11. Example of the E_{EMF} anomalies

Conclusion

A new form of the two measurement systems discussed was proposed. The results presented here demonstrate the effectiveness of the developed model of neural network architecture, based on a variational autoencoder (VAE) using LSTM layers and positional encoding. Thanks to these techniques, it was possible to achieve satisfactory values of metrics, which confirms the effectiveness of the approach used.

The solution proved particularly useful in the context of increasing the dataset by supplementing it with generalized time series. By generating additional data, it was possible to create precise ranges of variation for specific time moments, especially during key flight phases such as takeoff and landing. A modified PPA method was used for this purpose.

The generated data models allow efficient comparison of the new time courses, which in turn makes it possible to detect and analyze possible irregularities in the maneuvers performed. It has been shown that this type of solution has potential applications primarily in pilot training, since the takeoff and landing phases of an aircraft are among the most critical and risky.

The developed method can significantly contribute to improving flight safety, especially in the context of training, providing a tool for early detection of deviations from the norm in the time courses, which can lead to better analysis and optimization of flight maneuvers.

Authors: *dr inż. Joanna Michałowska, Faculty of Electrical Engineering and Computer Science, Lublin University of Technology, Lublin, Nadbystrzycka 38A, 20-618 Lublin, e-mail:j.michalowska@pollub.pl: dr inż. Paweł Tomiło, Faculty of Management, Lublin University of Technology, Lublin, Nadbystrzycka 38, 20-618 Lublin, e-mail:p.tomilo@pollub.pl;*

REFERENCES

[1] Suleman M., Gas P., Analytical, Experimental and Computational Analysis of Heat Released from a Hot Mug of Tea Coupled with Convection, Conduction, and Radiation Thermal Energy Modes, *International Journal of Heat and Technology*, (2024), vol. 42, no. 2, 359–372, doi: 10.18280/ijht.420201

[2] Gas P., Miaskowski A., Influence of the radiofrequency applicators arrangement on the sizes of ablative zones inside hepatic tumor, *Archives of Electrical Engineering*, (2024), 73 (3), 557-571, doi: 10.24425/aee.2024.150883
[3] Mazurek P., Michałowska J., Kozieł J., Gad R., Wdowiak A., The intensity of the electromagnetic fields in the coverage of GSM 900, GSM 1800 DECT, UMTS, WLAN in built-up areas, *Applications of Electromagnetics in Modern Techniques and Medicine*, PTZE (2018), 159 – 162, doi: 10.1109/PTZE.2018.8503156
[4] Kochan, O., Sapojnyk, H., & Kochan, R., Temperature field control method based on neural network, *In 2013 IEEE 7th International Conference on Intelligent Data Acquisition and Advanced Computing Systems (IDAACS)*, (2013), 1, 21-24, doi: 10.1109/IDAACS.2013.6662632
[5] Jiang, K., Zhang, C., Wei, B., Li, Z., & Kochan, O., Fault diagnosis of RV reducer based on denoising time–frequency attention neural network, *Expert Systems with Applications*, 238, (2024), doi: 10.1016/j.eswa.2023.121762
[6] Pytka J., Budzyński P., Tomiło P., Michałowska J., Błażejcza, D., Gnapowsk E., Pytka, J., Gierczak, K., *Measurement of aircraft ground roll distance during takeoff and landing on a grass runway*, *Measurement*, (2022), 10.1016/j.measurement.2022.111130
[7] Michałowska J., Tomiło P., Measurement System of an Electromagneric Field for Alircrafts with the Use of Machine Learning Model, *Metrology and Measurement System*, (2024), doi: 10.24425/mms.2024.150289
[8] Tomilo P., Classification of the Condition of Pavement with the Use of Machine Learning Methods, *Transport and Telecommunication*, (2023), 24 (2), 158 - 166, doi: 10.2478/ttj-2023-0014
[9] Leleń M., Biruk-Urban K., Jozwik J., Tomilo P., Modeling and Machine Learning of Vibration Amplitude and Surface Roughness after Waterjet Cutting, *Material*s,(2023), 16 (19), doi.10.3390/ma16196474
[10] Sun, L., Qin, H., Przystupa, K., Cui, Y., Kochan, O., Skowron, M., & Su, J., A hybrid feature selection framework using improved sine cosine algorithm with metaheuristic techniques, *Energies*, (2022), 15 (10), doi: 10.3390/en15103485
[11] Kingma Google, D.P., Welling M., Delft B., An Introduction to Variational Autoencoders. *Foundations and Trends R in Machine Learning*, (2019), doi:10.1561/2200000056
[12] Lindemann B., Müller T., Vietz H., Jazdi N., Weyrich M., A Survey on Long Short-Term Memory Networks for Time Series Prediction, *Procedia CIRP* (2021), 99, 650–655, doi:10.1016/J.PROCIR.2021.03.088.
[13] Chunkai Zhang, Yingyang Chen, Ao Yin, Zhen Qin, Xing Zhang, Keli Zhang, Zoe L. Jiang, An Improvement of PAA on Trend-Based Approximation for Time Series, *Springer*, (2018), doi: 10.48550/arXiv.1907.00700
[14] Diederik P. Kingma, Max Welling, An Introduction to Variational Autoencoders, *Now Foundations and Trends*, (2019), doi:10.1561/2200000056